Rydberg state creation by tunnel ionization

2013 New J. Phys. 15 013001

(http://iopscience.iop.org/1367-2630/15/1/013001)

New Journal of Physics
The open access journal for physics

Rydberg state creation by tunnel ionization

A S Landsman[1], A N Pfeiffer, C Hofmann, M Smolarski, C Cirelli and U Keller

Physics Department, ETH Zurich, CH-8093 Zurich, Switzerland
E-mail: landsmaa@ethz.ch

New Journal of Physics **15** (2013) 013001 (12pp)
Received 2 October 2012
Published 3 January 2013
Online at http://www.njp.org/
doi:10.1088/1367-2630/15/1/013001

Abstract. It is well known from numerical and experimental results that the fraction of Rydberg states (excited neutral atoms) created by tunnel ionization declines dramatically with increasing ellipticity of laser light, in a way that is similar to high harmonic generation (HHG). We present a method to analyze this dependence on ellipticity, deriving a probability distribution of Rydberg states that agrees closely with experimental (Nubbemeyer *et al* 2008 *Phys. Rev. Lett.* **101** 233001) and numerical results. We show using analysis and numerics that most Rydberg electrons are ionized before the peak of the electric field and therefore do not come back to the parent ion. Our work shows, for the first time, the similarities and differences in the process that distinguishes formation of Rydberg electrons from electrons involved in HHG: ionization occurs in a different part of the laser cycle, but the post-ionization dynamics are very similar in both cases, explaining why the same dependence on ellipticity is observed.

[1] Author to whom any correspondence should be addressed.

Contents

1. Introduction

Tunnel ionization, which can occur when an ionizing laser field strength is comparable to the Coulomb force binding the outer electron to its atom, is behind many recent breakthroughs marking this decade of attosecond science [2]. The three-step semiclassical model, which neglects the Coulomb force after ionization, works surprisingly well in explaining many phenomena, most notably high harmonic generation (HHG) [3]. More recently, the role of the Coulomb force in laser ionization has drawn considerable attention from the strong field atomic physics community. In particular, it is believed that to properly study other phenomena (e.g. focusing [4, 5], low-energy structures at mid-infrared wavelengths [6, 7], certain asymmetries in momentum spectra [8, 9], tunneling geometry [10] and, most notably for our analysis, the generation of Rydberg states [1, 11]), the inclusion of the Coulomb force is essential. Here, we show that a semiclassical model that neglects Coulomb force during the laser pulse explains recent experimental observations in the setting of elliptically polarized light, without the need to account for recollisions.

Rydberg states can be created when the tunneled electron does not gain sufficient energy from the laser pulse and is subsequently captured by the Coulomb field, creating an excited neutral atom. The mechanism behind Rydberg state creation has attracted much interest, with some of the first measurements, in the context of strong field ionization, in [12, 13]. Intermediate Rydberg states have been used to explain the formation of narrow peaks characteristic of multi-photon ionization [12], and as a probe of the spatial gradient of the pondermotive potential in a focused laser beam [14]. In [13], it was found that Rydberg atoms are not produced in circularly polarized light. This observation was recently confirmed in [1], where the Rydberg yield as a function of laser ellipticity, ϵ, was measured, showing the disappearance of excited neutrals above $\epsilon \approx 0.3$.

While some progress has been made in analyzing the generation of Rydberg states in linearly polarized light [11, 15], the role of polarization, and in particular the dramatic decline of Rydberg neutral atoms with increasing ellipticity of light, remains to be explained. Nubbemeyer *et al* [1] placed Rydberg states created via tunnel ionization in the same group as other 'tunneling-plus-rescattering' phenomena such as HHG, noting the same dependence on ellipticity as what is 'expected for a rescattering process'. However, the physical mechanism that determines whether the electron will be involved in HHG or be captured in a Rydberg state was not elucidated. In this work, we show that the distinguishing feature is the part of the laser

cycle where ionization takes place. In particular, Rydberg electrons are predominantly created before the peak of the laser field, while electrons that take place in HHG are ionized after the peak. This means that, unlike in HHG and other rescattering processes, most Rydberg electrons do not return to the tunnel exit. However, the initial velocity when a Rydberg electron emerges in the continuum is found to satisfy the same constraints as electrons involved in HHG. This explains the similar dependence of electron yield on ellipticity.

2. Analysis of the mechanism behind Rydberg state creation

2.1. The semiclassical model

The electric field of a laser propagating in the z-direction is given by

$$\vec{F}(t) = \frac{-F_0 f(t)}{\sqrt{\epsilon^2+1}}[\cos(\omega t+\phi_c)\,\hat{x} + \epsilon \sin(\omega t+\phi_c)\,\hat{y}], \tag{1}$$

where ω is the frequency of the laser, ϵ is the ellipticity (the major axis of polarization is along $\hat{x}$), and $f(t)$ is the slowly varying pulse envelope: $f_{\max} = f(0) = 1$. For many-cycle pulses, we can approximate the carrier-envelope offset (CEO) phase [16]: $\phi_c \approx 0$.

To lowest order, the electron dynamics following tunnel ionization are given in atomic units by [3]: $\partial^2\vec{r}/\partial t^2 = -\vec{F}(t)$. This simple equation is based on the assumption within the strong field approximation [3, 17] that the Coulomb force after ionization is negligible compared to the laser field: $|\vec{F}| \gg Q/r$. For the evaluation of Rydberg states, which by definition depend on the Coulomb potential, we will therefore only neglect the Coulomb force until the end of the laser pulse. After the laser pulse has passed, for $t \gg \tau_p/2$ (where τ_p is the pulse duration), we have $f(t) \approx 0$, so that from equation (1): $\vec{F}(t) \approx 0$ and therefore the Coulomb force is no longer negligible compared to the laser field, capturing lower energy trajectories into Rydberg states.

For a slowly varying envelope, where $\mathrm{d}f(t)/\mathrm{d}t \ll \omega$, the force equation can be integrated to give approximate dynamics for electrons following ionization,

$$x(t) \approx \frac{F_0\,(1 - f(t)\cos(\omega t))}{\omega^2\sqrt{\epsilon^2+1}} + v_{x0}t + x_e, \tag{2}$$

$$y(t) \approx \frac{\epsilon F_0\,(\omega\triangle t - f(t)\sin(\omega t))}{\omega^2\sqrt{\epsilon^2+1}} + v_y\triangle t; \quad z(t) \approx v_z\triangle t, \tag{3}$$

where $\triangle t = t - t_i$ (with t_i being the instance of ionization), and x_e is the exit point from the tunnel [3]. As an initial condition, we used $v_x(t_i) = 0$, in accordance with the tunneling model [3, 18]. The parallel velocity after the laser pulse has passed, v_{x0}, is determined by the phase of the field, ϕ_i, at the instance of ionization:

$$v_{x0} = -\phi_i F_0/\omega\sqrt{1+\epsilon^2}. \tag{4}$$

The transverse velocity at the exit point is given by (v_y, v_z) and has a Gaussian probability distribution given by the well-known ADK formula [18], with standard deviation:

$$\sigma_\perp = \sqrt{\omega/2\gamma}, \tag{5}$$

where γ is the Keldysh parameter: $\gamma = \omega\sqrt{2I_p}/F$.

Equation (2) shows that an electron that tunnels before the peak, where $v_{x0} > 0$ (see equation (4)), will continue, when averaged over a single cycle, to get farther from the exit

point during the duration of the pulse. In particular, this means that if Rydberg electrons are created predominantly before the peak of the laser field, they will not recollide with the parent atom, but will end up relatively far from the exit point, after the pulse has passed. Due to the low final momentum constraint on Rydberg electrons, we expect that they will be ionized in a time interval just before the peak of the laser field, since electrons formed near the peak of the field will have low final momentum at the detector. Our numerical simulations, see section 3, confirm that the ionization takes place shortly before the peak of the electric field.

2.2. Derivation of the Rydberg yield as a function of ellipticity of laser light

The overall structure of the following derivation for the Rydberg yield is as follows. We show that the electrons end up far from the exit point, x_e, after the laser pulse has passed. This imposes a near-zero final momentum condition. While the momentum along x is close to zero due to ionization near the peak, the final transverse momentum at the exit point needs to cancel out the drift velocity created by the laser field. Therefore, the probability of a Rydberg state can be obtained from the probability that the transverse velocity at the exit point (which is given by the ADK formula [18, 22]) is such that it approximately cancels the deterministic drift velocity.

From equation (2), the position of the electron ionized near the peak after the pulse has passed is

$$x_f = \frac{F_0}{\omega^2\sqrt{\epsilon^2+1}} + x_e \sim \frac{F_0}{\omega^2}. \tag{6}$$

The right-hand side of the equation holds for small ϵ and in the framework of the strong field infrared laser physics where $F_0/\omega^2 \gg x_e$.

From equation (6), it is clear that, in contrast to ionization by a plane wave, an electron ionized near the peak of a laser pulse will end up a significant distance from the parent atom after the laser pulse has passed. Since the distance from the parent atom at the end of the pulse is large, $x_f \gg x_e$, the velocity has to be small to satisfy the negative energy condition: $-Q/x_f + \mathrm{KE} \leqslant E < 0$ necessary for Rydberg states. Here $E = -Q/r + \mathrm{KE}$, and KE is the kinetic energy of the electron. We therefore require that the transverse velocity of the electron after the pulse has passed satisfies the following condition:

$$\tilde{v}_y = v_y + v_{\mathrm{drift}} \approx 0, \tag{7}$$

where $\tilde{v}_y$ was obtained from equation (3), and

$$v_{\mathrm{drift}} = \epsilon F_0/\omega\sqrt{\epsilon^2+1} \tag{8}$$

is the drift velocity caused by the vector potential of the laser field [3, 17].

From equation (5), the scaled probability of generating an electron with $v_y \approx -v_{\mathrm{drift}}$, satisfying equation (7), is

$$P_R(\epsilon) \approx P_0 \exp\left(-\frac{F_0(2I_p)^{1/2}}{\omega^2}\epsilon^2\right), \tag{9}$$

where P_0 is the ionization probability in the tunneling regime along the major axis of polarization [19].

The same dependence on parameters as in the above equation was recently found in the context of HHG [20]. This same dependence on parameters, both in Rydberg states and in HHG, is due to the condition that, in both cases, the initial transverse electron velocity must

cancel out the drift due to the vector potential of the field. However, as we confirm in section 3, other details of the dynamics are different, most notably the phase of the electric field where ionization takes place.

In the range of small ϵ, equation (9) can be approximated to exponential accuracy as: $P_0 = \exp(-2(2I_p)^{3/2}\sqrt{1+\epsilon^2}/3F_0)$ [21, 27]. The exponent of P_0 can be further Taylor expanded to obtain

$$P_R(\epsilon) \approx \mathrm{e}^{\frac{-2(2I_p)^{3/2}}{3F_0}} \mathrm{e}^{-\epsilon^2/2\sigma_\epsilon^2}, \tag{10}$$

where σ_ϵ is the standard deviation of the Gaussian probability distribution for the Rydberg state yield as a function of ellipticity of light:

$$\sigma_\epsilon = \sqrt{\frac{3}{3+\gamma^2}} \frac{\omega}{\sqrt{2F_0}\left(2I_p\right)^{1/4}}. \tag{11}$$

In deriving equation (10) a Taylor expansion was used, retaining only terms up to the order of ϵ^2, since $\epsilon^2 \ll 1$ (the Rydberg state generation is only found at small values of ϵ). In the tunneling regime where $\gamma \ll 1$, equation (11) can be approximated as

$$\sigma_\epsilon = \omega/\sqrt{2F_0}(2I_p)^{1/4}. \tag{12}$$

The standard deviation given in equation (11) increases with decreasing F_0, predicting a slower decline of Rydberg states with ϵ, as the laser intensity goes down. This is in contrast to the total ionization yield, given by P_0, where smaller laser intensities lead to a faster decline with ellipticity. These two factors lead to an increase of Rydberg trajectories relative to the total ionization yield, explaining and quantifying the findings in [1], where numerics show 'an increasing percentage of bound trajectories ... with decreasing laser intensity'.

2.3. Comparison of analytic results to experimental data

A comparison between the experimental data (taken from [1]), semiclassical simulations and the analytically obtained curve given by equation (10) is shown in figure 1. The intensity and laser frequency used in the figure were chosen for the purposes of comparison with the experiment in [1]. While the total ion yield varies slowly with increasing ellipticity, the yield of Rydberg states drastically decreases to essentially zero for $\epsilon > 0.3$. This holds true over a wide span of intensities (3.5×10^{14}–3×10^{15} W cm^{-2}), where analysis (see equation (10)) and numerics show the disappearance of Rydberg states in the $0.2 < \epsilon < 0.3$ range, depending on field strength.

Our experiment, first presented in [23], records electron momenta distributions at the detector. Here, we use the same experimental results, but display the energy, rather than momenta, of the electrons as a function of ellipticity, as shown in figure 2. This provides indirect information on Rydberg state generation by measuring the yield of $E \approx 0$ states at the detector as a function of ϵ. This is because the cut-off for $E \approx 0$ states also corresponds to the cut-off for Rydberg states, given by the condition $E = -1/2n^2 < 0$, where n is the quantum number.

The experimental setup was as follows. A laser of pulse duration (full-width at half-maximum) $\tau_p = 33$ fs, central wavelength $\lambda_0 = 788$ nm and peak intensity of 8×10^{14} W cm^{-2} (the CEO phase [16] was not stabilized) was produced by a Ti:sapphire laser system focused onto helium atoms in a cold gas jet, with the gas jet density adjusted such that on average

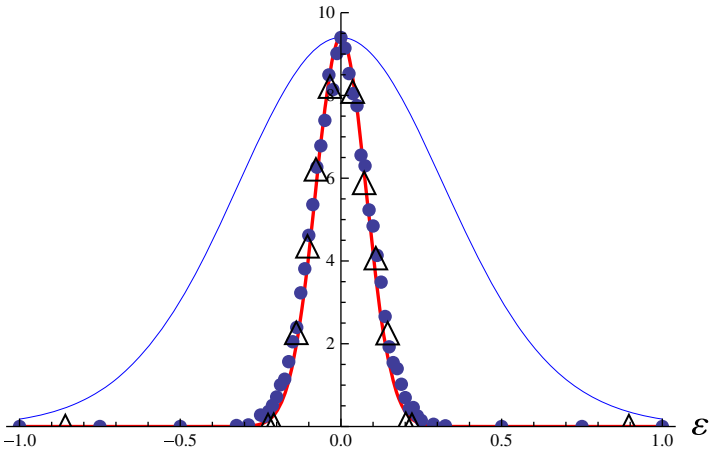

Figure 1. Analytic curve (red line), simulations (•) and experimental data (Δ) for the Rydberg yield. Total ion yield of He^+, given by P_0, is shown on the same plot (blue line). Experimental data are taken from [1]. $\tau_p = 30$ fs, $\omega = 0.056$ au and intensity $= 10^{15}$ W cm^{-2}, corresponding to $F_0 = 0.167$ au.

much less than one ionization occurs per laser shot. Note that these experimental parameters are similar in pulse duration, frequency and laser intensity to those used in figure 1.

A COLTRIMS setup [24] measures the ion momentum, which is the negative of the electron momentum due to momentum conservation. The momentum resolution is 0.1 au in the time-of-flight direction and 0.9 au in the gas jet direction, mainly determined by thermal spread. A broadband quarter-wave plate is used to alter the ellipticity of the laser pulses. In the final analysis, the ellipticity and the angular orientation of the polarization ellipse are calculated from the angle of the quarter-wave plate, respecting its wavelength dependence [26]. The knowledge of the ellipticity and the angle of the polarization ellipse for each detected ion allow generation of ellipticity-resolved spectra with a high resolution.

These experimental results are presented in figure 2. The figure shows that $E \approx 0$ states decline dramatically and virtually disappear for $\epsilon > 0.3$, in agreement with theory and numerics, shown in figure 1, which also predict the disappearance of Rydberg states close to $\epsilon \approx 0.3$.

The abrupt decrease of Rydberg states with ellipticity, shown in figure 1, is also typical of a rescattering process as measured for HHG and non-sequential multiple ionization (NSMI) [1, 20, 25]. However, note that, unlike HHG and NSMI, a typical Rydberg trajectory does not come back to the parent atom after ionization. This is fully supported by our detailed semiclassical simulations, as described in the next section.

3. Simulations of Rydberg trajectories

Our analytic results indicate that Rydberg trajectories occur when the transverse velocity at the exit point cancels out the drift momentum of the laser field. This results in the ellipticity dependence shown in figure 1. However, the same type of ellipticity dependence occurs in HHG [1, 20]. To better understand what distinguishes Rydberg electrons from electrons that come back to the parent ion, in a process of HHG or NSMI, we perform detailed Monte Carlo simulations.

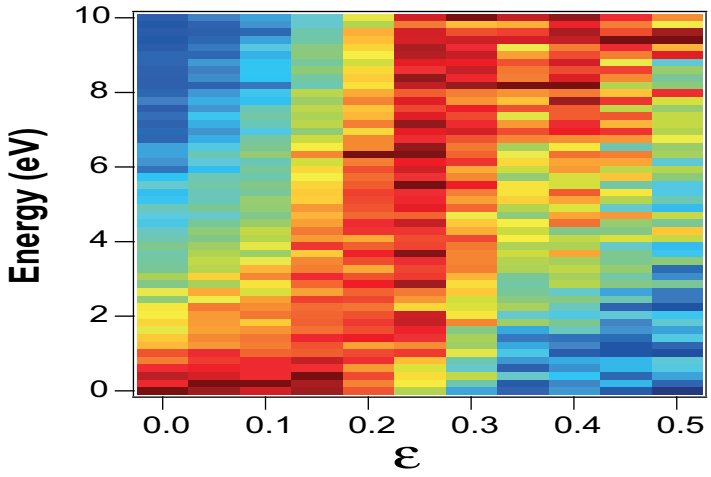

Figure 2. Energy of electrons observed at the detector as a function of ellipticity of laser light. $\tau_p = 33$ fs, $\lambda_0 = 788$ nm and intensity $= 8 \times 10^{14}$ W cm^{-2}.

Monte Carlo simulations were performed whereby an ensemble of 3×10^5 ionization events was generated for each value of ϵ over the interval $[-0.44, 0.44]$. For each ensemble, the distribution of ionization phases, $\phi_i = \omega t_i$, was given by the instantaneous electric field within the strong-field approximation, $P(\phi_i) \propto \exp(-2(2I_p)^{3/2}/3F(t_i))$, and assuming instantaneous tunneling delay time [24]. To approximate the Coulomb potential due to the parent ion, a soft core potential [1] was used. The equations of motion were solved with an initial condition that the electron starts its trajectory outside the potential barrier, at the exit point, x_e, which was obtained using parabolic coordinates [10], with an initial longitudinal momentum of zero, in accord with the tunneling model, and a transverse momentum distribution given by equation (5). A cosine-squared envelope was used with a pulse duration of 30 fs. All trajectories were evaluated at the end of the pulse, with Rydberg trajectories (i.e. trajectories satisfying $E < 0$) saved, to establish the phase at ionization and the fraction of rescattering events.

The results of these simulations are shown in figures 3, 4 and 6 for a laser frequency and duration similar to experiments in [1] and [23]. The peak field strength of $F_0 = 0.1$ au, corresponding to an intensity of 3.56×10^{14} W cm^{-2}, is also well within the experimental range explored in [1]. Figure 3 shows that most Rydberg electrons do not come back to the exit point after ionization. This is in agreement with prior findings for linearly polarized light, showing that Rydberg electrons are ionized before the peak of the laser pulse and therefore avoid 'hard recollisions' [15]. The fraction of rescattered electrons increases with decreasing ellipticity, but stays below about 15% of the total Rydberg trajectories. As explained in section 2.1, the fact that a high fraction of Rydberg electrons do not come back to the parent atom suggests that most ionization events take place before the peak of the electric field. To confirm this, we found the fraction of Rydberg electrons ionized before the peak as a function of ellipticity, with the results shown in figure 4. Interestingly, while most electrons appear before the peak for all values of ϵ, their relative percentage drops as ellipticity increases. At the same time, as figure 3 shows, the fraction of Rydberg electrons which do not rescatter increases with ϵ. This indicates that at higher ellipticities, a greater fraction of Rydberg electrons come back to the parent ion along the direction of ionization, but avoid recollision due to significant transverse displacement caused by the greater drift momentum, given in equation (8).

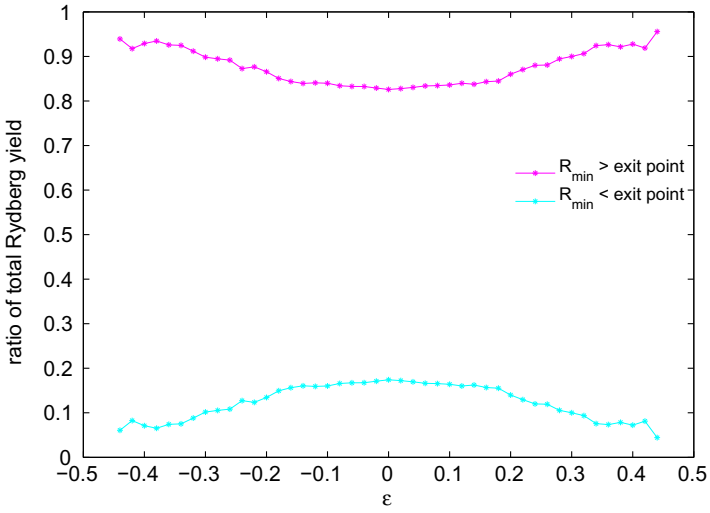

Figure 3. Monte Carlo simulations showing the fraction of Rydberg electrons that do not rescatter (top curve) and electrons that do rescatter (bottom curve) as a function of ellipticity. Rescattering is defined as coming back to the exit point of the parent atom. $F_0 = 0.1$ au (or intensity $= 3.56 \times 10^{14}$ W cm^{-2}), $\omega = 0.0578$ au.

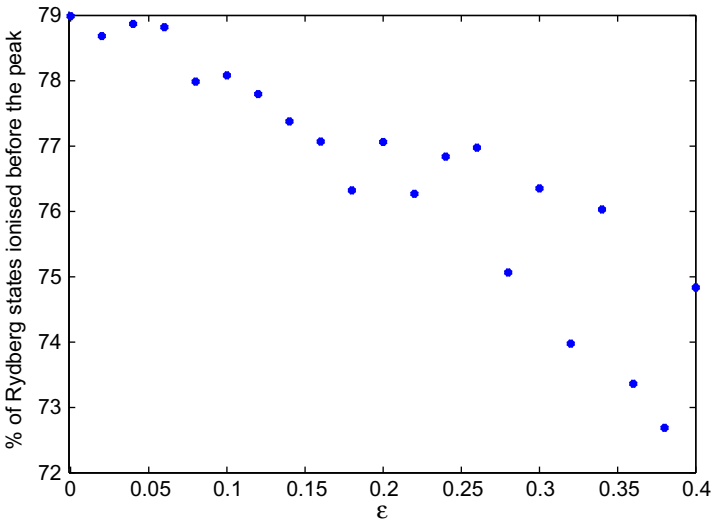

Figure 4. Percentage of Rydberg electrons that appeared in the continuum before the peak of the laser field, for different values of ellipticity. All parameters are the same as in figure 3.

The interplay between the initial momentum and the phase of the electric field at ionization is shown in figure 5 for different values of ellipticity. The figure was obtained by using equations (2) and (3) and calculating the range of initial conditions that satisfied the $E < 0$ constraint after the end of the laser pulse. The initial conditions corresponding to electrons that become trapped into Rydberg states are contained within the solid line curves shown in figure 5. All these curves are centered around the value of the initial velocity that exactly

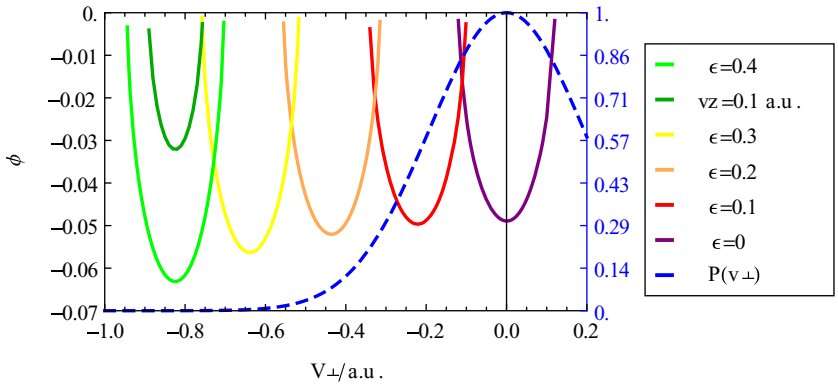

Figure 5. The allowed range of ionization phases and initial velocities for Rydberg trajectories for different ellipticities. All Rydberg electrons must have initial conditions inside the parabolic domains. The blue dashed line shows transverse velocity probability distribution, with standard deviation given by equation (5). The dark green curve includes an initial velocity in the direction of propagation of $v_z = 0.1$ au, with $\epsilon = 0.4$, like in the light green curve.

cancels the final drift momentum, given by equation (8). As can be seen from figure 5, the range of initial velocities allowed for Rydberg trajectories expands as ionization occurs closer to the peak, located at $\phi = 0$. This can be understood by considering that the total final energy of the Rydberg electron has to satisfy $E < 0$, so that if the final momentum in the direction of ionization is larger, as happens when the ionization time moves to earlier before the peak, then the allowed range of initial transverse momenta is smaller. As the broken line in figure 5 indicates, the probability of having the required initial velocity to generate a Rydberg state for a given value of ϵ is very low for $\epsilon \geqslant 0.3$. Having a velocity component in the direction of laser propagation (along the z-axis) further constrains the allowed range of initial velocities in the plane of polarization, as shown by the dark green curve in figure 5.

We also checked the ionization phase of the 'most probable' Rydberg trajectory as a function of ellipticity, shown in figure 6. Interestingly, at lower ellipticities, the ionization occurs earlier before the peak of the electric field, corresponding to a higher momentum in the direction of ionization at the end of the laser pulse. This further confirms that electrons at lower ϵ can have a larger displacement along the direction of ionization, since they have a smaller displacement along the transverse direction, compared to the higher ϵ case. This suggests that although post-ionization dynamics of Rydberg trajectories are subject to the same constraints on transverse velocity as electrons involved in recollisions and HHG, these constraints are somewhat more 'flexible', allowing for some interchange between transverse and longitudinal displacements. Such an interchange is impossible in the case of a recollision, where an electron must return to the parent ion, both in the direction of ionization and in transverse directions.

4. Discussion

We analyzed the dependence of Rydberg states on laser ellipticity, deriving a Gaussian probability distribution for the yield of excited neutral atoms as a function of ϵ. Our results indicate that Rydberg electrons have transverse velocities at the tunnel exit comparable to the

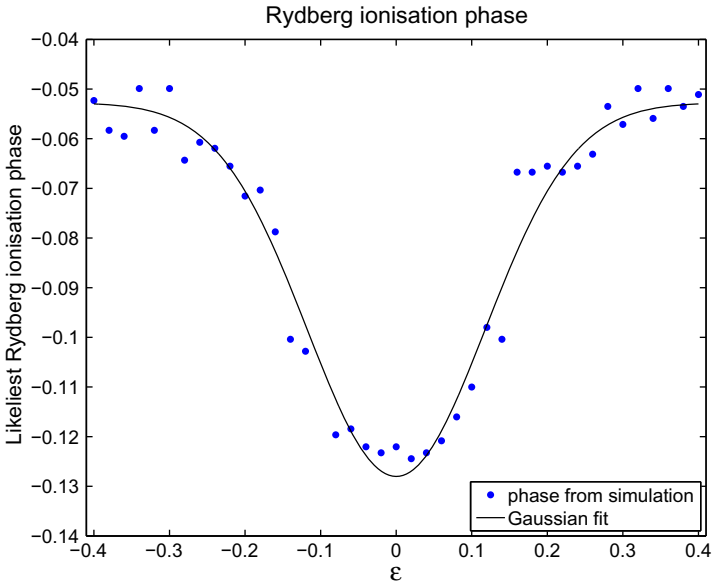

Figure 6. The most probable ionization phase for the Rydberg trajectory, as a function of ellipticity of laser light. All parameters are the same as in figure 3.

electrons involved in HHG [28], due to the same requirement for the initial velocity to cancel the final drift momentum. This results in a dependence of Rydberg trajectories on ellipticity, see equation (9), that is the same, to the lowest order, as that found in HHG [20].

As a result of common initial conditions at the tunnel exit, there are certain common features shared by these two rather distinct processes. In particular, as equations (9)–(12) indicate, increasing the frequency of the laser light should result in a slower decline of Rydberg states with ellipticity. The same behavior was recently found for HHG, where it was shown that the decrease of high harmonic yield for a 400 nm laser pulse was about 1.5 times slower than for the 800 nm [20]. The higher conversion efficiency found at shorter wavelengths for HHG therefore also applies to enhancing the yield of neutral Rydberg atoms. It would be particularly interesting to experimentally investigate how Rydberg states can be populated by short infrared, for example 10 μm, pulses [29]. The standard deviation of the Rydberg yield probability distribution, given by equation (11), is found to decrease with increasing laser intensity. However, the overall ionization probability, given by P_0 in equation (9), increases with increasing intensity. A possible solution, as suggested in [29], is to use molecules where the ionizing laser field can be small but the ionization yield large because of enhanced ionization [30].

In contrast to HHG, Rydberg electrons are created predominantly before the peak of the electric field. This means that most electron trajectories do not come back near the exit point of the parent atom. Also, the initial condition constraints on Rydberg electrons are less severe than those on electrons involved in HHG. For instance, a small but non-negligible fraction of Rydberg trajectories appears in the continuum after the peak of the electric field, and therefore comes back to the parent atom along the direction of ionization, but avoids recollision due to transverse displacement. In contrast, in HHG, the electron has to return to the parent atom along the direction of ionization as well as the transverse directions. This places a greater constraint on the possible range of initial conditions, presumably resulting in curves narrower than those

shown in figure 5. This could also explain the lower percentage of recolliding electrons [11, 31] as compared to the Rydberg yield, which was measured at around 10% [1].

Our results also indicate that a shorter pulse length is more effective in enhancing the yield of Rydberg neutrals [29], in agreement with numerical results in [1]. This can be understood by considering the distance of the electron from the parent atom after the laser pulse has passed. Since there should be some small, but non-zero, initial velocity, the electron will be found further from the atom at the end of the pulse for longer pulses and hence is less likely to be captured.

The experimental data presented here confirm the disappearance of Rydberg states for $\epsilon > 0.3$ by measuring zero energy states at the detector. These states can be considered as a cut-off for the creation of bound trajectories since they correspond to asymptotically large values of n (the quantum number of the Rydberg state). From the above discussion it seems clear that this cut-off can be moved to higher values of ϵ, and the yield of neutral Rydberg atoms can be enhanced if few-cycle pulses of shorter infrared wavelength are used.

Acknowledgments

We gratefully acknowledge Dr Eichmann for providing us with the experimental data displayed in figure 1 (see [1]). This work was supported by the NCCR Quantum Photonics (NCCR QP) and NCCR Molecular Ultrafast Science and Technology (NCCR MUST), research instruments of the Swiss National Science Foundation (SNSF), ETH Research under grant no. ETH-03 09-2 and an SNSF equipment grant. ASL is supported by the FP7 IIF under grant no. 275313.

References

[1] Nubbemeyer T, Gorling K, Saenz A, Eichmann U and Sandner W 2008 *Phys. Rev. Lett.* **101** 233001
[2] Krausz F and Ivanov M 2009 *Rev. Mod. Phys.* **81** 163
[3] Corkum P B 1993 *Phys. Rev. Lett.* **71** 1994
[4] Brabec T, Ivanov M Y and Corkum P B 1996 *Phys. Rev.* A **54** R2551
[5] Comtois D *et al* 2005 *J. Phys. B: At. Mol. Opt. Phys.* **38** 1923
[6] Blaga C I *et al* 2009 *Nature Phys.* **5** 335
[7] Liu C P and Hatsagortsyan K Z 2010 *Phys. Rev. Lett.* **105** 113003
[8] Bashkansky M, Bucksbaum P H and Schumacher D W 1988 *Phys. Rev. Lett.* **60** 2458
[9] Goreslavski S P, Paulus G G, Popruzhenko S V and Shvetsov-Shilovski N I 2004 *Phys. Rev. Lett.* **93** 233002
[10] Pfeiffer A N *et al* 2012 *Nature Phys.* **8** 76–80
[11] Yudin G L and Ivanov M Y 2001 *Phys. Rev.* A **63** 033404
[12] de Boer M P and Muller H G 1992 *Phys. Rev. Lett.* **68** 2747
[13] Jones R R, Schumacher D W and Bucksbaum P H 1993 *Phys. Rev.* A **47** R49
[14] Wells E, Ben-Itzhak I and Jones R R 2004 *Phys. Rev. Lett.* **93** 023001
[15] Shvetsov-Shilovski N I *et al* 2009 *Laser Phys.* **19** 1550
[16] Telle H R *et al* 1999 *Appl. Phys.* B **69** 327
[17] Ivanov M Y, Spanner M and Smirnova O 2005 *J. Mod. Opt.* **52** 165
[18] Ammosov M V, Delone N B and Krainov V P 1986 *Sov. Phys.—JETP* **64** 199
[19] Keldysh L V 1965 *J. Exp. Theor. Phys.* **20** 1307
[20] Khan S D *et al* 2011 *Appl. Phys. Lett.* **99** 161106
[21] Perelomov A M, Popov V S and Terent'ev M V 1966 *J. Exp. Theor. Phys.* **50** 1393
[22] Tong X M and Lin C D 2005 *J. Phys. B: At. Mol. Opt. Phys.* **38** 2593

[23] Pfeiffer A N, Cirelli C, Landsman A S, Smolarski M, Dimitrovski D, Madsen L B and Keller U 2012 *Phys. Rev. Lett.* **109** 083002
[24] Eckle P *et al* 2008 *Science* **322** 1525
[25] Dietrich P, Burnett N H, Ivanov M and Corkum P B 1994 *Phys. Rev.* A **50** R3585
[26] Smolarski M *et al* 2010 *Opt. Express* **18** 17640
[27] Popov V S 2004 *Phys.—Usp.* **47** 855–85
[28] Shafir D, Soifer H, Bruner B D, Dagan M, Mairesse Y, Pathkovskii S, Ivanov M Y, Smirnova O and Dudovich N 2012 *Nature* **485** 343
[29] Corkum P B 2012 private communication
[30] Seideman T, Ivanov M Y and Corkum P B 1995 *Phys. Rev. Lett.* **75** 2819
[31] Klaiber M, Kohler M C, Hatsagortsyan K Z and Keitel C H 2012 *Phys. Rev.* A **85** 063829